APPLIED SCIENCES AND ENGINEERING

Acoustic tweezer with complex boundary-free trapping and transport channel controlled by shadow waveguides

Junfei Li[1], Chen Shen[1,2], Tony Jun Huang[3], Steven A. Cummer[1]*

Acoustic tweezers use ultrasound for contact-free, bio-compatible, and precise manipulation of particles from millimeter to submicrometer scale. In microfluidics, acoustic tweezers typically use an array of sources to create standing wave patterns that can trap and move objects in ways constrained by the limited complexity of the acoustic wave field. Here, we demonstrate spatially complex particle trapping and manipulation inside a boundary-free chamber using a single pair of sources and an engineered structure outside the chamber that we call a shadow waveguide. The shadow waveguide creates a tightly confined, spatially complex acoustic field inside the chamber without requiring any interior structure that would interfere with net flow or transport. Altering the input signals to the two sources creates trapped particle motion along an arbitrary path defined by the shadow waveguide. Particle trapping, particle manipulation and transport, and Thouless pumping are experimentally demonstrated.

INTRODUCTION

Acoustic tweezers use ultrasound to create radiation force potential wells that enable precise and contact-free manipulation of physical and biological objects across a broad object size range (1–5). It is a fast-developing platform that finds applications in a wide range of fields, including chemical reaction control, microrobotics, drug delivery, and cell and tissue engineering. For example, acoustic tweezers have attracted much attention as they are capable of performing noncontact, label-free, and precise manipulation of bioparticles in a microfluidic chamber (2, 3, 4, 6). They have been applied to different scenarios such as cell patterning and printing (7–12), cell separation and sorting (13–15), tissue engineering (16–20), and isolating extracellular vesicles (21).

To date, the vast majority of acoustic tweezers in microfluidic chambers rely on arrays of transducers that surround the chamber to generate standing waves that form acoustic traps in a periodic pattern (1, 6, 7, 10, 11, 15). Such standing waves not only preclude particle selectivity by generating a large number of stable trapping points but also substantially constrain the overall spatial distribution of trapping points. The ability to better control the forces inside the chamber to form more complex or arbitrary particle trapping patterns in a selective manner with acoustic tweezers is highly desirable.

At least three different approaches have been previously applied to gain that additional control. The first is to create physical boundaries inside the trapping chamber for additional particle confinement. These boundaries include microfluidic channels (21) or hydrogel fibers (16) to confine the particles along narrow, predefined paths, and then use standing waves to maneuver particles inside this channel. However, for micro- and nanoscale devices, the solid walls of these fluid channels can limit achievable flow rates, and friction with the walls can trap or destroy the particle. Furthermore, such

devices are prone to fouling and clogging. Sheath flow can be actively generated to help avoid solid walls but requires a continuous flow of the central liquid and the surrounding liquid (22), which adds to system complexity and thus limits applications. The second approach is to develop sources capable of projecting a more complex sound field into the interior of the chamber. For example, a selective, single-point acoustic tweezer can be achieved by projecting a focused acoustic vortex at the focal plane in the microfluidic chamber (23) using specially designed spiral transducers. However, this method cannot easily create more complex trapping paths or points, and particle manipulation requires the mechanical motion of the source.

The third approach to control the acoustic fields inside the microfluidic chamber is to design engineered structures on or near the chamber boundary that influence the acoustic field locally in ways that cannot easily be done with exterior sources. One such example controls the sound field by patterning a phononic crystal structure on the chamber boundary, which can enable manipulation of droplets (24), fluids (25), and particles (26–28). However, using a phononic crystal structure also has some key limitations, namely, a narrow operating frequency range, required structural uniformity over large regions, and limited control over the configuration of trapping or transport channels. Nevertheless, local structure can control acoustic fields with high precision and in ways not easily done with source arrays, and this approach remains relatively unexplored.

This paper presents a boundary structure approach for controlling wave fields and propagation inside an open chamber through thin, broadband structures that are completely exterior to the chamber. These structures act as a virtual waveguide that tightly confines the acoustic field along a complex path inside the microfluidic chamber. We call this a "shadow waveguide" since no physical boundary is present inside the chamber, but the acoustic fields, particle trapping, and particle transport closely follow the external structure. Through the shadow waveguide, we demonstrate in both simulations and experiments a highly selective acoustic tweezer that traps and manipulates particles along a thin, single predefined but complex path through the chamber. Such a waveguide design is inherently broadband, which greatly enriches the versatility of acoustic tweezers

[1]Department of Electrical and Computer Engineering, Duke University, Durham, NC 27708, USA. [2]Department of Mechanical Engineering, Rowan University, Glassboro, NJ 08028, USA. [3]Department of Mechanical Engineering and Materials Science, Duke University, Durham, NC 27708, USA.
*Corresponding author. Email: cummer@ee.duke.edu.

by unlocking arbitrary and complex input waves that form the acoustic trap. As an example, we demonstrate precise control of the position and velocity of trapped particles by frequency detuning two sources to form potential wells moving at a controlled speed, analogous to Thouless pumping (29) for quantized charge transport. The mode shape in the shadow waveguide can be engineered to accommodate particles with both positive and negative acoustic contrasts. The design is easy to fabricate and could find utility in a range of biomedical and chemical applications.

RESULTS
Device principle and design
At the interface between two media with different refractive indices, total internal reflection occurs when the incident angle is above the critical angle. Wave propagation can thus be confined along a narrow channel by wrapping a high index material (the core) with a low index material (the cladding). Such a mechanism serves as the basis for optical fibers and silicon photonics. Our strategy relies on an acoustic version of such waveguides, as shown in Fig. 1. We use structured polydimethylsiloxane (PDMS) and glass plates to form a quasi–two-dimensional (2D) microfluidic open chamber. PDMS is used because it is a water-like material with low shear modulus and is easy to fabricate. A designed air-PDMS structure is formed between the

PDMS and the bottom plate. The PDMS-air interface acts as a soft boundary, so the water and PDMS structure (a ridge in this case) together form a waveguide that supports propagating modes through multiple reflections. The effective refractive index can be controlled by the height of the PDMS layer. Thicker PDMS results in slower effective sound speed in the water chamber. Therefore, the acoustic wave field inside the chamber is guided by the PDMS structure that is fully outside the chamber. Hence, particles in the microfluidic chamber can be trapped and manipulated along an arbitrarily shaped and narrow channel without any physical boundary inside the chamber.

Simulation of the acoustic fields in the shadow waveguide
The acoustic field is analyzed by the full-wave eigenfrequency simulation through COMSOL Multiphysics. The mode shape of the shadow waveguide is shown in Fig. 1B. The detailed geometric parameters can be found in the Supplementary Materials. The black curve denotes the pressure distribution along the PDMS-water interface. We can see that the wave is tightly confined in the core and decays exponentially away from the center. This shadow waveguide design traps and manipulates negative acoustic contrast particles that are attracted to pressure maxima. The corresponding dispersion relation is shown in Fig. 1C. The linear dispersion indicates that such a shadow waveguide supports a wide range of frequencies with the same group velocity. This broadband property can be exploited for
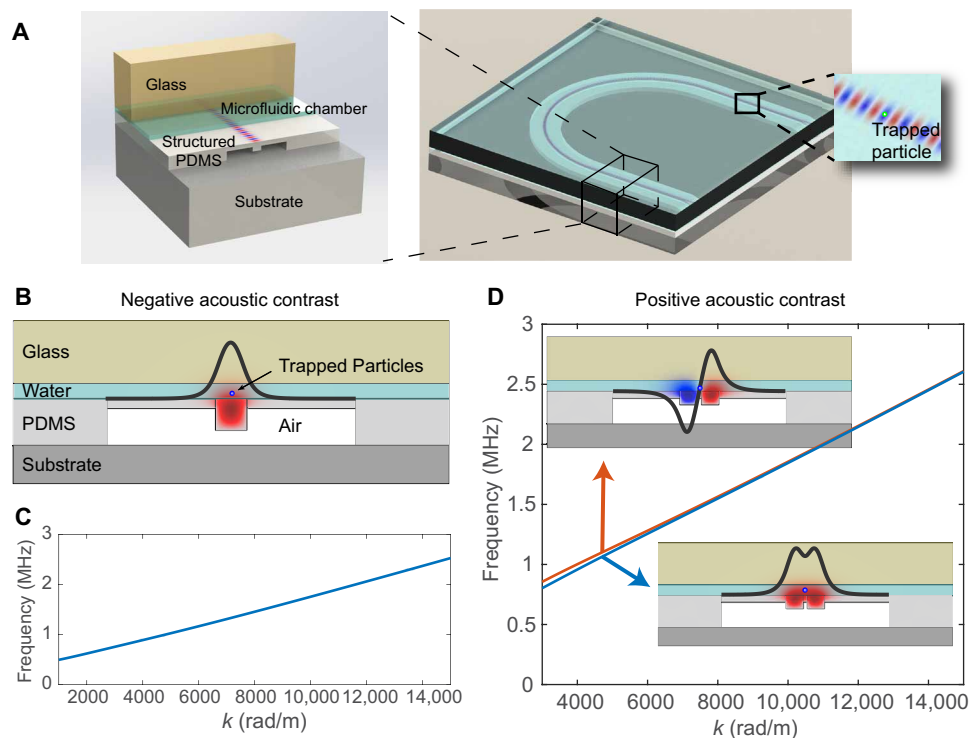

Fig. 1. Illustration and properties of the microfluidic chamber and shadow waveguide. (**A**) Glass plates and a layer of structured polydimethylsiloxane (PDMS) bound the microfluidic chamber. The acoustic field in the microfluidic chamber is controlled through a structure from the outside that we call a shadow waveguide. The particles in the microfluidic chamber are constrained by the shadow waveguide fields and can thus be confined and manipulated without a physical boundary. (**B**) Cross-sectional view shows the mode shape of a shadow waveguide designed to trap negative acoustic contrast particles. The PDMS structure forms regions with a certain effective index profile to guide the waves. The black line shows the pressure amplitude distribution along the water-PDMS interface. The acoustic field inside the microfluidic chamber is controlled by structures from outside, and the mode is highly localized. (**C**) Linear dispersion of the shadow waveguide allows it to guide a wide range of frequencies. (**D**) Different structures, such as a coupled parallel waveguide, can be designed to engineer the mode shapes for manipulating particles with positive acoustic contrast that are trapped by local pressure minima. The inset shows the pressure distribution of the first two modes.

the generation of complex potential profiles in both space and time, which can, in turn, lead to sophisticated control of particles and more capable acoustic tweezers.

Coupled waveguide design for positive contrast particles

In biomedical applications, many particles, such as cells, have a positive acoustic contrast and thus are attracted to pressure minima. The shadow waveguide design can be modified to accommodate these particles by creating local pressure minima through mode shape engineering. Here, we present a design composed of two coupled waveguides with two degenerate modes with local pressure minima: symmetric and antisymmetric modes. The geometry, simulated mode shapes, and corresponding pressure distributions are shown in the inset of Fig. 1D. By controlling the geometrical parameters, the mode shape can thus be engineered to create a local minimum with controlled width and depth, where particles with positive contrast can be trapped and manipulated.

Experimental demonstration

Experiments validate the capabilities of the shadow waveguide acoustic tweezer. The setup and photograph of samples are shown in Fig. 2 (A and D). Two lead zirconate titanate (PZT) transducers (15 mm by 20 mm by 2.1 mm; resonant frequency, 1 MHz) serve as sources. In the first case, single-frequency waves are generated by both transducers with a function generator (RIGOL DG4102) and amplified by power amplifiers. PDMS lenses focus and couple the incident waves into the waveguide. Details about the lens design can

be found in the Supplementary Materials. The PDMS layer is tapered at both ends to enhance the coupling into a guided mode. A standing wave pattern is created along the path of the shadow waveguide. Colored PDMS particles with sizes smaller than 150 μm are fabricated and dispensed in the chamber. In the experiment, the input power for both sources is 2.69 W, consistent with previous literature. When the source is turned on, the particles are rapidly concentrated to the pressure antinodes (movie S1). To calculate the trapping stiffness, we simulated the field distribution inside the microfluidic chamber with the measured power input and then calculated the radiation forces with the Gor'kov theory (30). The trapping stiffness is then calculated by taking the derivative of the forces in the transverse (x) direction and propagation (y) direction, reaching $k_x = 0.0243$ N/m and $k_y = 0.3793$ N/m, respectively. The shadow waveguide works for both straight and curved thin channels, as demonstrated in Fig. 2 (B and E). Figure 2 (C and F) shows the corresponding simulated pressure amplitude distributions at the same length scale. The correspondence between acoustic field and particle positions can be clearly seen. By adjusting the relative phase between two transducers, a standing wave inside the shadow waveguide can trap and move the particles along a predefined path in the open microfluidic chamber without a solid boundary (movie S2).

The experimental demonstration of a coupled waveguide system for manipulating particles with positive acoustic contrast is shown in Fig. 2 (G to I). In this case, we used polyamide particles with a diameter of 60 μm. An interesting result is that the particles not only are trapped along the center of the waveguide but also aligned
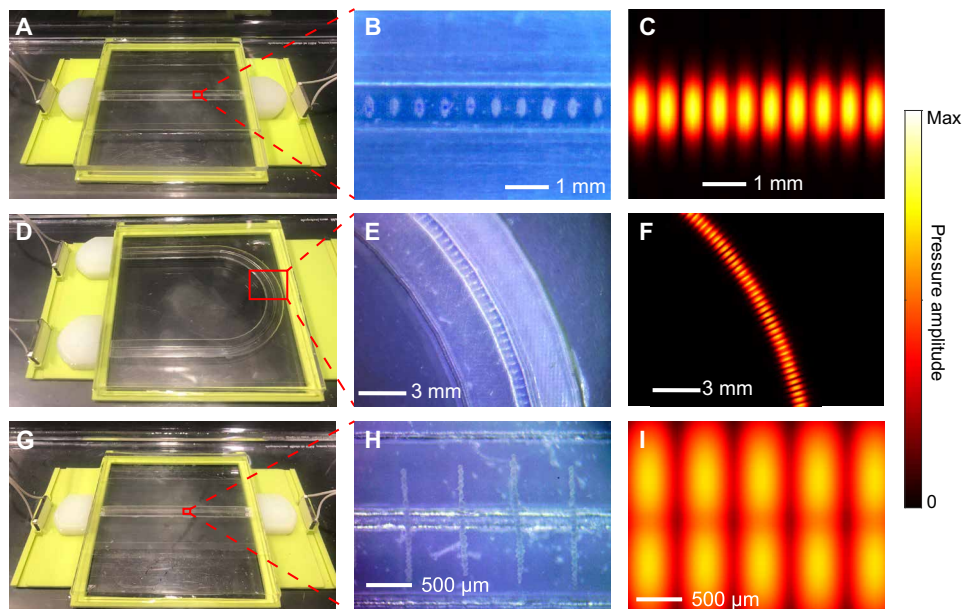

Fig. 2. Experimental setup and particle manipulation with shadow waveguide acoustic tweezers. (**A**) Photograph of the fabricated device. A PDMS lens is designed to couple the plane wave generated by the piezoelectric ceramic into the microfluidic chamber. (**B**) Negative contrast (PDMS) particle concentration and manipulation along a straight shadow waveguide (see movies S1 and S2). (**C**) The corresponding simulated pressure amplitude at the PDMS-water interface. (**D** to **F**) Photograph, experimental particle image, and simulated pressure distribution of a shadow waveguide to manipulate particles along a curved path. (**G** to **I**) Coupled shadow waveguide for manipulating polyamide particles with positive acoustic contrast. The anisotropic potential well can not only trap and move particles but also align them within the trap. By controlling the standing wave ratio, the anisotropic potential well can be tuned. We emphasize that while the shadow waveguide structure can be seen in the images (B, E, and H) through the transparent glass and water, that structure is completely outside the chamber (see Fig. 1, A and B). Photo credit: Junfei Li, Duke University.

themselves inside each potential well. This is achieved by controlling the standing wave ratio and the depth of local minima in the fundamental mode, so that the particles experience an anisotropic radiation force, where the pressure gradient in the transverse direction is smaller than that in the propagation direction. The ratio between these two forces can be further tuned by adjusting the input standing wave ratio, as we show in the Supplementary Materials.

Thouless pump for particles

A Thouless pump (29, 31) enables the robust transport of charge through an adiabatic cyclic evolution of the underlying Hamiltonian, which has attracted tremendous attention in the quantum world (31–34). We show that such a concept can also be realized in acoustic tweezers to achieve robust, continuous transport of particles at a controlled speed. For theoretical simplicity, we first consider a 1D system with no dispersion. When two counter-propagating waves have slightly different frequencies, $\omega_{1,2} = \omega_0 \pm \delta\omega$ ($\delta\omega \ll \omega_0$), the resulting total field becomes

$$p = p_0 e^{j\left[(\omega_0+\delta\omega)t-\frac{\omega_0+\delta\omega}{c}x\right]} + p_0 e^{j\left[(\omega_0-\delta\omega)t+\frac{\omega_0+\delta\omega}{c}x\right]}$$
$$= 2p_0 e^{j\left(\omega_0 t-\frac{\delta\omega}{c}x\right)} \cos\left(\delta\omega t - \frac{\omega_0}{c}x\right) \qquad (1)$$

Here, the two waves have the same amplitude. Similar results can be found when the two waves have different amplitudes (see the Supplementary Materials for details). The resulting field shows a fast oscillating wave modulated by a slowly moving envelope. Such an envelope travels at a speed of $c\delta\omega/\omega_0$, much slower than the speed of sound in the medium, as demonstrated in Fig. 3A. The resulting Gor'kov potential (30) thus behaves like a Thouless pump that transports particles along the shadow waveguide path with a controlled and adjustable speed, as shown in movies S3 and S4 for the straight channel and U-shaped channel cases, respectively. Figure 3B shows the corresponding experimental image sequence in time, in good agreement with theoretical predictions. The speed of the propagating potential can be precisely controlled by tuning the amount of frequency detuning. Figure 3C shows the particle velocity under frequency detuning through both theoretical prediction and experimental measurements. At center frequency $f_0 = 1$ MHz, the phase speed in the waveguide calculated from simulation is $\omega/k = $

1304 mm/s. Experimental results show excellent agreement with the theoretical calculation, featuring a linear relationship between the pumping speed and amount of detuning. The small discrepancy can be attributed to the fabrication error and imperfect clock in the function generator.

DISCUSSION

In summary, we have demonstrated an acoustic tweezer capable of generating a highly confined and selective trapping path of almost arbitrary spatial complexity inside an open chamber without any interior structure. The spatial pattern of the acoustic field is controlled by shadow waveguide structure completely exterior to the chamber and creates a trapping and transport geometry that would be exceedingly difficult to generate only through sources on the chamber boundary. By engineering the mode shape inside the shadow waveguide, manipulation of particles with both positive and negative contrasts along predefined narrow and complex paths is demonstrated experimentally.

The shadow waveguide approach brings some advantages and possibilities to acoustic tweezers. Compared with conventional acoustic tweezers that use an array of sources to create standing wave patterns along Cartesian or cylindrical coordinates, shadow waveguides guide acoustic waves in more versatile and selective spatial distributions and thereby achieve 2D and quasi-3D particle manipulation along complicated paths with only one pair of transducers. Although a predefined path limits the capability of free-form manipulation of objects, reconfigurable devices can be designed by introducing active elements to the shadow structure. In addition, the particles can be confined to a single thin path without the existence of a physical boundary. A shadow waveguide thus circumvents some of the drawbacks of physical microfluidic channels such as limited flow rates for a given pressure drop and the need for sheath flow to prevent particle jamming. Such a feature can potentially be used for nondestructive cell sorting and transport at high throughput. The lack of physical boundary with the shadow waveguide approach also allows interaction and information exchange between the trapped particles, such as cells and bacteria, and their environment. In addition, compared with previous efforts to control
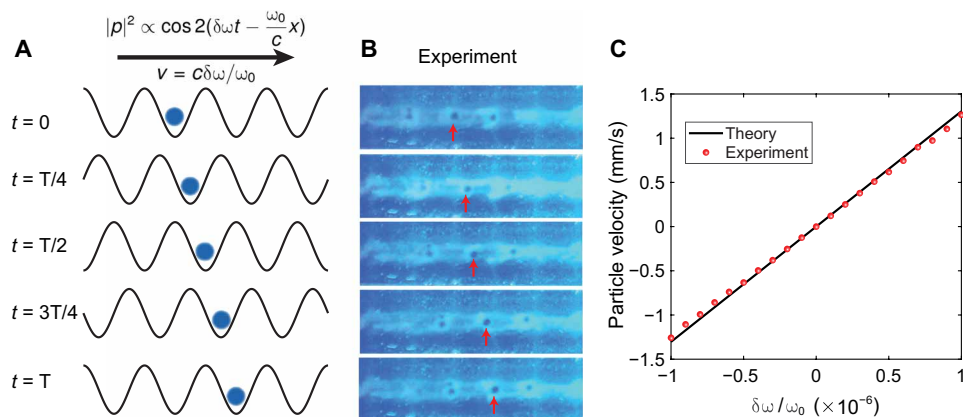

Fig. 3. Experimental demonstration of a Thouless pump in a microfluidic chamber. (**A**) A Thouless pump uses a potential that changes in both space and time to manipulate particles captured in it. The speed can be precisely controlled by synthesizing the desired potential field. (**B**) A time series of experimental photographs showing how particles are pumped in one cycle. (**C**) The pumping speed is linearly proportional to the frequency detuning of the input fields. Experimental particle velocity shows good agreement with the theoretical prediction.

sound propagation in microfluidic chambers using phononic crystals, shadow waveguides allow a much wider range of guided mode shapes with little dispersion, unlocking the possibility of more advanced particle manipulation. As a demonstration of this, a coupled parallel shadow waveguide with a mode shape designed for manipulating particles with positive acoustic contrast was shown. We would also like to note here that our device is more closely aligned with bulk wave acoustic tweezers (35). Such a technique potentially enables large and cost-effective piezo elements to be used for high-precision manipulation as the sound is directed to exactly where it is needed. The concept of wave manipulation with shadow structures is also expected to benefit surface acoustic wave devices.

Broadband shadow waveguides also enable the creation of complex time-varying acoustic actuation. As an example, we demonstrated a Thouless pump along a prescribed channel in a completely open chamber using two counter-propagating waves at different frequencies. The resulting time-varying potential wells can pump particles at a precisely controlled speed, which is expected to enable precisely controlled cell transport, counting, and controlled chemical syntheses. Designing more complex time-varying functionalities by synthesizing the potential input fields is possible with a systematic approach to synthesize arbitrary time-dependent potential wells for acoustic tweezers. Also, the mode shape engineering demonstrated in this work represents a small fraction of what is possible. By designing the effective index profile in the shadow structure, other forms of wave manipulation devices can potentially be created, enabling more versatile functionalities such as cell sorting, concentration, and centrifugation. Nevertheless, the shadow waveguide approach for designing acoustic tweezer functionality presented in this work provides advantages over existing systems and opens up new possibilities for designing advanced acoustic tweezers for a range of biomedical and chemical applications.

MATERIALS AND METHODS
Device fabrication and setup
The PDMS layer is fabricated with the standard PDMS molding process. A negative mold was fabricated with stereolithography 3D printing and treated with trichloro (Sigma-Aldrich) vapor in a vacuum chamber for 1 hour. Parts A and B of PDMS (QSIL 216) are mixed thoroughly by a 10:1 weight ratio, degassed in a vacuum chamber, and then poured into the mold. The mold is degassed and then baked in an oven at 120°C for an hour for the silicone to cure (36). The PDMS is then separated from the mold and attached to the glass plate to form the shadow waveguide.

PDMS microparticle fabrication
We fabricated microparticles of PDMS (QSIL 216) inspired by the procedure in (37). PDMS base (premixed with blue ink) and curing agent are mixed thoroughly by a 10:1 weight ratio and added to a water bath with 1 weight % nonionic surfactant poly(ethylene glycol)-block-poly(propylene glycol)-block-poly(ethylene glycol) (Sigma-Aldrich). The emulsion was heated at 70°C and continuously agitated using a mixer for an hour. The cooled mixture then passes through a 100-mesh sieve to keep particles smaller than 150 μm.

Numerical simulations
The mode shape is analyzed through eigenfrequency simulation in COMSOL Multiphysics, Pressure Acoustics module. Perfect matching layers are used on the left and right sides of the simulation domain. An out-of-plane wave number is assigned and then the eigenmodes are solved by finding the eigenfrequency around an estimated value. Then, we swept the out-of-plane wave number to calculate the ω − k diagram.

SUPPLEMENTARY MATERIALS

REFERENCES AND NOTES
1. S. Oberti, A. Neild, J. Dual, Manipulation of micrometer sized particles within a micromachined fluidic device to form two-dimensional patterns using ultrasound. *J. Acoust. Soc. Am.* **121**, 778–785 (2007).
2. J. Friend, L. Y. Yeo, Microscale acoustofluidics: Microfluidics driven via acoustics and ultrasonics. *Rev. Mod. Phys.* **83**, 647–704 (2011).
3. A. Ozcelik, J. Rufo, F. Guo, Y. Gu, P. Li, J. P. Lata, T. J. Huang, Acoustic tweezers for the life sciences. *Nat. Methods* **15**, 1021–1028 (2018).
4. P. Li, T. J. Huang, Applications of acoustofluidics in bioanalytical chemistry. *Anal. Chem.* **91**, 757–767 (2019).
5. L. Meng, F. Cai, F. Li, W. Zhou, L. Niu, H. Zheng, Acoustic tweezers. *J. Phys. D Appl. Phys.* **52**, 273001 (2019).
6. D. J. Collins, B. Morahan, J. Garcia-Bustos, C. Doerig, M. Plebanski, A. Neild, Two-dimensional single-cell patterning with one cell per well driven by surface acoustic waves. *Nat. Commun.* **6**, 8686 (2015).
7. J. Shi, D. Ahmed, X. Mao, S.-C. S. Lin, A. Lawit, T. J. Huang, Acoustic tweezers: Patterning cells and microparticles using standing surface acoustic waves (SSAW). *Lab Chip* **9**, 2890–2895 (2009).
8. L. Meng, F. Cai, Z. Zhang, L. Niu, Q. Jin, F. Yan, J. Wu, Z. Wang, H. Zheng, Transportation of single cell and microbubbles by phase-shift introduced to standing leaky surface acoustic waves. *Biomicrofluidics* **5**, 044104 (2011).
9. F. Gesellchen, A. Bernassau, T. Déjardin, D. R. S. Cumming, M. Riehle, Cell patterning with a heptagon acoustic tweezer–application in neurite guidance. *Lab Chip* **14**, 2266–2275 (2014).
10. F. Guo, Z. Mao, Y. Chen, Z. Xie, J. P. Lata, P. Li, L. Ren, J. Liu, J. Yang, M. Dao, S. Suresh, T. J. Huang, Three-dimensional manipulation of single cells using surface acoustic waves. *Proc. Natl. Acad. Sci. U.S.A.* **113**, 1522–1527 (2016).
11. Z. Tian, S. Yang, P. Huang, Z. Wang, P. Zhang, Y. Gu, H. Bachman, C. Chen, M. Wu, Y. Xie, T. J. Huang, Wave number–spiral acoustic tweezers for dynamic and reconfigurable manipulation of particles and cells. *Sci. Adv.* **5**, eaau6062 (2019).
12. Z. Tian, Z. Wang, P. Zhang, T. D. Naquin, J. Mai, Y. Wu, S. Yang, Y. Gu, H. Bachman, Y. Liang, Z. Yu, T. J. Huang, Generating multifunctional acoustic tweezers in Petri dishes for contactless, precise manipulation of bioparticles. *Sci. Adv.* **6**, eabb0494 (2020).
13. M. Antfolk, C. Magnusson, P. Augustsson, H. Lilja, T. Laurell, Acoustofluidic, label-free separation and simultaneous concentration of rare tumor cells from white blood cells. *Anal. Chem.* **87**, 9322–9328 (2015).
14. D. J. Collins, B. L. Khoo, Z. Ma, A. Winkler, R. Weser, H. Schmidt, J. Han, Y. Ai, Selective particle and cell capture in a continuous flow using micro-vortex acoustic streaming. *Lab Chip* **17**, 1769–1777 (2017).
15. L. Ren, S. Yang, P. Zhang, Z. Qu, Z. Mao, P.-H. Huang, Y. Chen, M. Wu, L. Wang, P. Li, T. J. Huang, Standing surface acoustic wave (SSAW)-based fluorescence-activated cell sorter. *Small* **14**, 1801996 (2018).
16. J. P. Lata, F. Guo, J. Guo, P.-H. Huang, J. Yang, T. J. Huang, Surface acoustic waves grant superior spatial control of cells embedded in hydrogel fibers. *Adv. Mater.* **28**, 8632–8638 (2016).
17. C. Bouyer, P. Chen, S. Güven, T. T. Demirtas, T. J. F. Nieland, F. Padilla, U. Demirci, A bio-acoustic levitational (BAL) assembly method for engineering of multilayered, 3D brain-like constructs, using human embryonic stem cell derived neuro-progenitors. *Adv. Mater.* **28**, 161–167 (2016).
18. B. Kang, J. Shin, H.-J. Park, C. Rhyou, D. Kang, S.-J. Lee, Y. Yoon, S.-W. Cho, H. Lee, High-resolution acoustophoretic 3D cell patterning to construct functional collateral cylindroids for ischemia therapy. *Nat. Commun.* **9**, 5402 (2018).
19. J. P. K. Armstrong, J. L. Puetzer, A. Serio, A. G. Guex, M. Kapnisi, A. Breant, Y. Zong, V. Assal, S. C. Skaalure, O. King, T. Murty, C. Meinert, A. C. Franklin, P. G. Bassindale, M. K. Nichols, C. M. Terracciano, D. W. Hutmacher, B. W. Drinkwater, T. J. Klein, A. W. Perriman, M. M. Stevens, Engineering anisotropic muscle tissue using acoustic cell patterning. *Adv. Mater.* **30**, 1802649 (2018).
20. X. Wang, L. Tian, Y. Ren, Z. Zhao, H. Du, Z. Zhang, B. W. Drinkwater, S. Mann, X. Han, Chemical information exchange in organized protocells and natural cell assemblies with controllable spatial positions. *Small* **16**, 1906394 (2020).

21. M. Wu, Y. Ouyang, Z. Wang, R. Zhang, P.-H. Huang, C. Chen, H. Li, P. Li, D. Quinn, M. Dao, S. Suresh, Y. Sadovsky, T. J. Huang, Isolation of exosomes from whole blood by integrating acoustics and microfluidics. *Proc. Natl. Acad. Sci. U.S.A.* **114**, 10584–10589 (2017).

22. P. Tabeling, *Introduction to Microfluidics* (OUP Oxford, 2005).

23. M. Baudoin, J.-C. Gerbedoen, A. Riaud, O. B. Matar, N. Smagin, J.-L. Thomas, Folding a focalized acoustical vortex on a flat holographic transducer: Miniaturized selective acoustical tweezers. *Sci. Adv.* **5**, eaav1967 (2019).

24. Y. Bourquin, R. Wilson, Y. Zhang, J. Reboud, J. M. Cooper, Phononic crystals for shaping fluids. *Adv. Mater.* **23**, 1458–1462 (2011).

25. J. Reboud, Y. Bourquin, R. Wilson, G. S. Pall, M. Jiwaji, A. R. Pitt, A. Graham, A. P. Waters, J. M. Cooper, Shaping acoustic fields as a toolset for microfluidic manipulations in diagnostic technologies. *Proc. Natl. Acad. Sci. U.S.A.* **109**, 15162–15167 (2012).

26. F. Li, F. Cai, Z. Liu, L. Meng, M. Qian, C. Wang, Q. Cheng, M. Qian, X. Liu, J. Wu, J. Li, H. Zheng, Phononic-crystal-based acoustic sieve for tunable manipulations of particles by a highly localized radiation force. *Phys. Rev. Appl.* **1**, 051001 (2014).

27. F. Li, Y. Xiao, J. Lei, X. Xia, W. Zhou, L. Meng, L. Niu, J. Wu, J. Li, F. Cai, H. Zheng, Rapid acoustophoretic motion of microparticles manipulated by phononic crystals. *Appl. Phys. Lett.* **113**, 173503 (2018).

28. F. Li, F. Cai, L. Zhang, Z. Liu, F. Li, L. Meng, J. Wu, J. Li, X. Zhang, H. Zheng, Phononic-crystal-enabled dynamic manipulation of microparticles and cells in an acoustofluidic channel. *Phys. Rev. Appl.* **13**, 044077 (2020).

29. D. J. Thouless, Quantization of particle transport. *Phys. Rev. B* **27**, 6083–6087 (1983).

30. L. P. Gor'kov, On the forces acting on a small particle in an acoustical field in an ideal fluid. *Dokl. Phys.* **6**, 773 (1962).

31. M. Switkes, C. M. Marcus, K. Campman, A. C. Gossard, An adiabatic quantum electron pump. *Science* **283**, 1905–1908 (1999).

32. Q. Niu, Towards a quantum pump of electric charges. *Phys. Rev. Lett.* **64**, 1812–1815 (1990).

33. M. Lohse, C. Schweizer, O. Zilberberg, M. Aidelsburger, I. Bloch, A Thouless quantum pump with ultracold bosonic atoms in an optical superlattice. *Nat. Phys.* **12**, 350–354 (2016).

34. S. Nakajima, T. Tomita, S. Taie, T. Ichinose, H. Ozawa, L. Wang, M. Troyer, Y. Takahashi, Topological Thouless pumping of ultracold fermions. *Nat. Phys.* **12**, 296–300 (2016).

35. B. W. Drinkwater, Dynamic-field devices for the ultrasonic manipulation of microparticles. *Lab Chip* **16**, 2360–2375 (2016).

36. J. Li, A. Crivoi, X. Peng, L. Shen, Y. Pu, Z. Fan, S. A. Cummer, Three dimensional acoustic tweezers with vortex streaming. *Commun. Phys.* **4**, 113 (2021).

37. K. Melde, A. G. Mark, T. Qiu, P. Fischer, Holograms for acoustics. *Nature* **537**, 518–522 (2016).

Citation: J. Li, C. Shen, T. J. Huang, S. A. Cummer, Acoustic tweezer with complex boundary-free trapping and transport channel controlled by shadow waveguides. *Sci. Adv.* **7**, eabi5502 (2021).